

# Some aspects of splat-quenching in an inert atmosphere and of the formation of non-crystalline phases in Al-17.3 at. % Cu, germanium and tellurium

H. A. DAVIES, J. B. HULL

*Department of Metallurgy, University of Sheffield, Sheffield, UK*

An apparatus for splat-quenching by the gun technique in a sealed, inert atmosphere is described. The importance of a low-oxygen quenching atmosphere in promoting efficient spreading of liquid particles and good thermal contact with the quenching surface is shown. A cooling rate of  $\sim 10^{10}$  K sec<sup>-1</sup> was estimated from the interlamellar spacing in a quenched Al-17.3 at. % Cu alloy. The process mechanisms of the gun technique are discussed with particular reference to the atomized droplet size and the effective specimen thickness for heat transfer.

New non-crystalline phases are reported in electron-transparent areas of splat-quenched foils of Al-17.3 at. % Cu (eutectic composition) pure Ge and pure Te. The glassy Al-Cu phase was also observed in specimens which were chemically thinned from the thicker regions of foils; lattice image studies by high-resolution electron microscopy tentatively suggest that this phase has an amorphous, liquid-like atomic configuration. The peak positions in the electron diffraction patterns of the Ge and Te phases were compared, where possible, with those for the corresponding liquid and vapour-deposited phases. The results for Ge suggest that significant structural rearrangement took place during cooling and freezing from the liquid to give a paracrystalline, tetrahedral short-range order whereas, for Te, the liquid structure was probably largely preserved on freezing.

## 1. Introduction

A particularly interesting feature of splat-quenching techniques is that they facilitate the formation in certain alloys of glassy phases in which non-crystalline structures are retained on solidification. Of the quenching techniques that have been devised, the original gun technique of Duwez and Willens [1] appears to give the highest average cooling rate, partly because of the efficient atomization and high velocity of impact of the molten specimen and the consequent thinness of the sample. The range of non-crystalline metallic materials that has been produced in this way is still, however, quite small, especially when compared with vapour-deposition techniques, for instance. Although there is little information available on glass transition temperatures in metallic materials, it is reasonable to suppose that, if the cooling rate of the splat-quenching technique could be

increased, a wider range of materials could be quenched into a non-crystalline form. Recent work in which a substantial increase in the thermal conductivity of the quenching surface resulted in the formation of an amorphous Al-Ge alloy [2] points to this. Although, in much of the previous splat-quenching work utilizing the gun technique, precautions have been taken to limit oxidation of the droplet, prior to atomization, less attention has generally been paid to minimizing oxidation during the atomization and quenching process which is the critical stage when a very large surface area/volume ratio is presented to the environment. Even a thin film of surface oxide is likely to adversely affect contact between the liquid and substrate and thus limit the maximum cooling rate obtainable. Recent studies in which the quenching was performed in an atmosphere of inert gas confirm this view [3]. Moreover, oxygen absorbed or

entrapped during quenching could influence the structure of the sample and give rise to spurious thermal effects during subsequent thermal studies of phase changes at elevated temperatures [4].

This paper describes a system which facilitates quenching in a sealed chamber, which can be evacuated prior to charging with inert gas. The results of initial experiments, in which the cooling rate was estimated and non-crystalline phases were produced in eutectic Al-Cu alloy, germanium and tellurium, are then discussed with particular reference to the process mechanism of the technique and the conditions required for metallic glass formation.

## 2. Apparatus

This is shown diagrammatically in Fig. 1. The

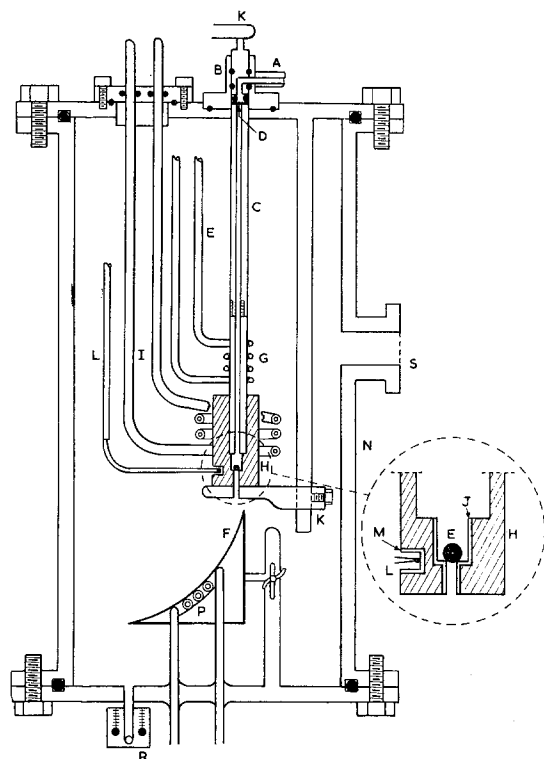


*Figure 1* Diagram of apparatus for splat-quenching in sealed inert atmosphere. *Key to parts:* A, high pressure gas inlet; B, high pressure chamber; C, shock tube; D, mylar diaphragm; E, molten sample; F, "ski slope" surface; G, cooling coil; H, graphite crucible; I, r.f. heating coil; J, alumina lining for sample chamber and orifice; K, clamp; L, Pt/Pt-Rh thermocouple; M, alumina lining for thermocouple well; N, steel chamber; P, cooling for quenching surface—water or liquid nitrogen; R, pressure release valve; S, port for diffusion pump and inert gas supply.

propelling device is similar to that of Duwez and Willens [1] except that the whole assembly is contained within a 150 mm i.d. cylindrical steel chamber, N, having removable top and bottom plates with "O"-ring seals. The shock tube, the leads to the induction coil, the sheathed thermocouple and the water-cooling coil pass through the top plate via "O"-ring seals. The quenching surface is mounted on the bottom plate, with provision for vertical, lateral and tilting adjustment. The copper tubing which carries the cooling medium (either flowing water or liquid nitrogen) is hard-soldered to the underside of the quenching surface and passes through the bottom plate via hard-soldered joints. A pressure release valve, R, is also incorporated into the bottom plate.

The flanged side-arm, S, is connected to vacuum pumps which facilitate evacuation of the vessel to a pressure below  $2 \times 10^{-5}$  Torr, prior to flushing with high-purity inert gas. The vacuum pumps also have access, through a high-pressure isolating valve, to the high pressure line in order to remove oxygen introduced when changing diaphragms.

The cavity at the bottom of the crucible, in which the molten sample is held prior to quenching, and the orifice through which it is ejected are lined with an insert of alumina, J, as shown in the expanded drawing. Temperature is measured by means of a Pt/Pt-Rh thermocouple, L, located in an alumina-lined cavity, M, adjacent to the specimen.

## 3. Results

### 3.1. Non-crystalline phase in Al-17.3 at. % Cu

Initial investigations were made on this alloy of eutectic composition with the intention of determining the maximum rate of cooling attainable, since it had previously been found applicable over a wide range of cooling rates [5]. Foils approximately 10 mm wide  $\times$  20 mm long, which were generally porous and of bulk thickness varying up to 20  $\mu$ m, were produced by quenching 100 mg droplets of the alloy from a temperature of  $750 \pm 10^\circ\text{C}$  on to the water-cooled copper surface; this surface was abraded with SiC paper prior to each quench in order to ensure it was clean and free of oxide and to promote good adhesion between it and the foil. Pressures up to 7 MN  $\text{m}^{-2}$  ( $\sim 1000$  psi) were employed to fracture the Mylar diaphragm and accelerate the molten droplet.

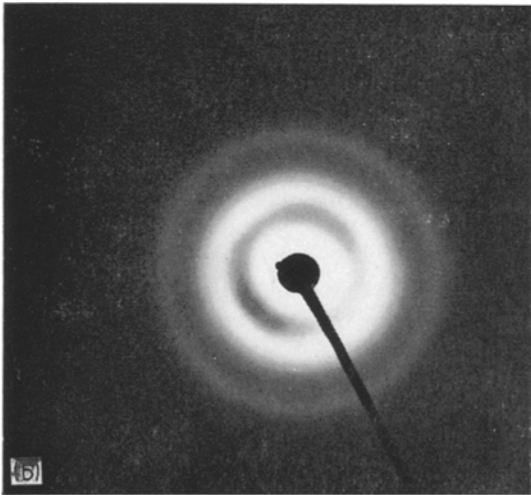


Figure 2 (a) Electron micrograph of non-crystalline phase in splat-quenched Al-17.3 at.% Cu ( $\times 80000$ ). (b) Electron diffraction pattern of same area.

Specimens were initially quenched in argon atmospheres, introduced after prior evacuation of the vessel to  $2 \times 10^{-5}$  Torr and flushing with the argon. The foils were examined by transmission electron microscopy with 100 kV and 1 MV instruments. The thinnest parts, particularly adjacent to the edges, were electron-transparent and, since the prime object was to study the effects that occurred in the regions which had cooled most rapidly, i.e. generally, though not in all cases, the thinnest regions, relatively few observations were made on

chemically thinned specimens taken from the thicker sections. Most of the 100 kV electron-transparent areas were found to be structureless at magnifications up to  $\times 120000$  (Fig. 2a). Selected-area diffraction patterns from these areas consisted of diffuse rings, characteristic of a non-crystalline phase [6] (Fig. 2b); the breadths of the rings were found to be comparable with those of amorphous splat-quenched Pd-18 at.%Si. The positions of the first two peaks, determined from microdensitometer traces of the pattern and expressed in terms of the diffraction co-ordinate  $K = 4\pi \sin \theta/\lambda$ , were 2.70 and  $4.93 \text{ \AA}^{-1}$ . The first peak position corresponds fairly closely with that of the (111) peak of the metastable Al-17.3 at.% Cu crystalline phase ( $2.75 \text{ \AA}^{-1}$ ).

Further studies were made on these structureless areas using a 100 kV microscope fitted with a high-resolution stage in which a lattice image formation method was employed at magnifications of  $\times 400000$  to  $\times 500000$ . This involves forming an interference micrograph between the transmitted beam and a portion of the first diffracted ring, governed by the aperture employed, using tilted illumination. If microcrystallites were present, straight fringes with the appropriate (111) layer spacing ( $\sim 2.4 \text{ \AA}$ ) should be observed running for distances corresponding to the microcrystallite size and in various directions corresponding to the angular range of the first diffracted ring accepted by the aperture. The plates were studied with a magnifier and printed with an enlargement of about  $\times 5$ , which



Figure 3 High resolution lattice image electron micrograph of non-crystalline phase in splat-quenched Al-17.2 at. % Cu ( $\times 250000$ ).

gave a linear resolution of about 2 Å. Such a micrograph is shown in Fig. 3. Through-focus series of pictures were taken of the same area and Fig. 3 represents the image as close to the focusing point as was possible to judge. No extended crystallites can be seen and the structure appears similar to that observed for a splat-cooled Cu-Zr alloy by Revcolevschi and Grant [7] using the same technique. In that case the structure was described as suggesting "atomic clusters 5 to 6 Å apart". Such a cluster size is so small as to have little meaning, especially in a material having close-packed non-directional bonding. Lattice image micrographs were also obtained from samples of sputtered and vapour-deposited germanium as a test of the technique and as a comparison; the structure was similar to that which had been reported previously [8] with groups of four or five straight fringes, suggesting microcrystallites of 14 to 20 Å diameter. On the present evidence, the non-crystalline splat-quenched Al-Cu phase could therefore be described as having an amorphous rather than microcrystalline structure, although a possible effect of this relatively thick specimen ( $\sim 0.1 \mu\text{m}$ ) in masking or distorting lattice fringes, due to overlapping effects, should not be ruled out. Further work would be desirable using smaller apertures to limit further

the angular range, and hence also the fraction, of the diffracting regions which contribute to the interference effect.

The formation of a non-crystalline phase on rapid quenching of this alloy was somewhat surprising since the eutectic in this system is not deep and neither of the components is a metalloid or non-metal, both of these factors having hitherto been considered to be important in promoting glass formation. A metastable solid-solution single phase having a fcc structure has been reported previously in a splat-quenched alloy of this composition [2]. In the present case of the non-crystalline phase, the crystallization of the fcc phase was evidently being suppressed and the maximum cooling rate was presumably higher than in the previous work. The formation of glassy phases is briefly discussed in Section 3.5.

### 3.2. Estimation of cooling rate

In a few individual quenched droplets at the edges of some foils, where the thermal contact was not as good as in other regions of the edge, a very fine lamellar-like structure was observed, with, in the case of the finest lamellae, an average spacing of approximately 8 nm (80 Å) (Fig. 4); a non-lamellar phase, probably supersaturated solid-solution, was sometimes associated with this, although positive identification by selected-area diffraction was not possible owing to the fineness and complexity of the overall microstructure.

Burden and Jones [5] have shown that the interlamellar spacing  $\lambda$  and the growth velocity,  $R$ , from this eutectic alloy can be satisfactorily related, over a wide range of growth velocities, as follows:

$$\lambda^2 R \approx 108 \mu\text{m}^3 \text{sec}^{-1}. \quad (1)$$

Assuming that conditions of Newtonian cooling apply, where the Nusselt number  $N < 0.015$  [9], the rate of cooling,  $r$ , can be expressed by:

$$r = \frac{RL_f}{Ct}$$

where  $L_f$  is the latent heat of fusion = 341 J g<sup>-1</sup>;  $C$  is the specific heat = 0.71 J g<sup>-1</sup> K<sup>-1</sup>;  $t$  is the splat thickness. Therefore, if it is assumed that relation 1 is valid for all rates of growth,

$$r = \frac{108 L_f}{\lambda^2 C t}.$$

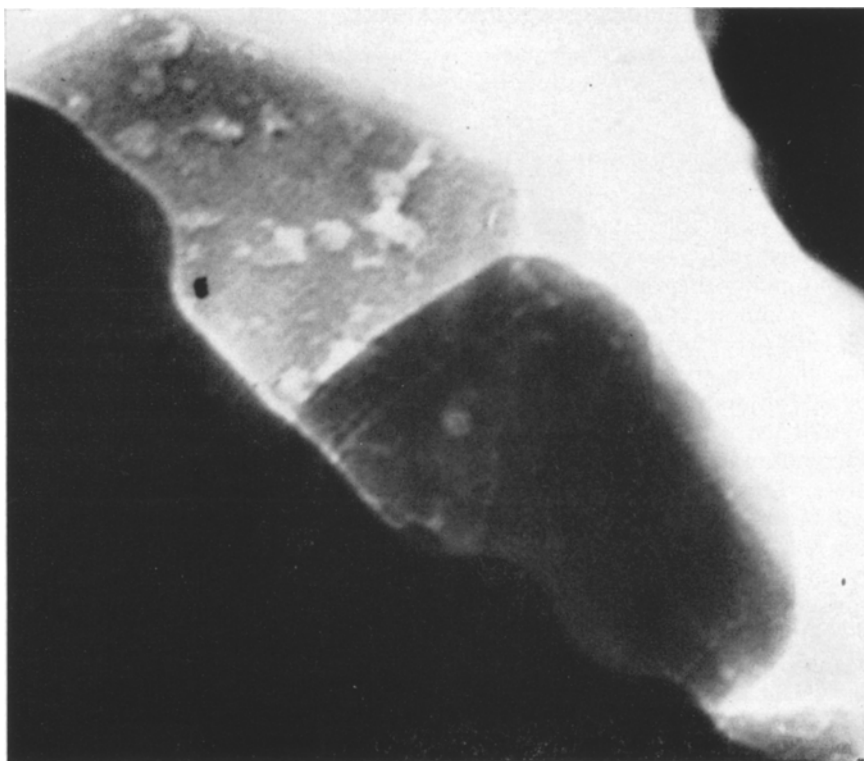


Figure 4 Electron micrograph of individual droplets from edge of splat-quenched Al-17.3 at. % Cu sample ( $\times 240000$ ).

For the electron-transparent areas of the present alloy, using 100 kV, the thickness is  $\leq 0.15 \mu\text{m}$ . On this basis, and assuming the duplex structure to be lamellar, the cooling rate is calculated to be  $\sim 10^{10} \text{ K sec}^{-1}$ . This is essentially a very approximate estimate in view of the uncertainties inherent in the calculation.

An assumption of intermediate or ideal cooling (where  $N > 0.015$ ), as opposed to Newtonian cooling, would give a higher calculated value of  $r$ .  $N$  is given by  $N = ht/k$  where  $k$  is thermal conductivity  $\approx 125 \text{ J m}^{-2} \text{ sec}^{-1} \text{ K}^{-1}$ ,  $h$  is heat transfer coefficient  $= \rho L_f R / (\theta_F - \theta_A)$ ,  $\rho$  is the density of the alloy  $\approx 3500 \text{ kg m}^{-3}$ ,  $\theta_F$  is the freezing temperature and  $\theta_A$  the substrate temperature. It is difficult to estimate the actual freezing temperature because of the probability of substantial undercooling. For the formation of the non-crystalline phase, the undercooling must be at least 400 K assuming a glass transition temperature of  $\sim 150^\circ \text{C}$ . However, for the lamellar product the undercooling is likely to be substantially less and we will assume that it is 150 K so that  $(\theta_F - \theta_A) \sim 400 \text{ K}$ .  $h$

will then be  $\sim 8.2 \times 10^6 \text{ J m}^{-2} \text{ K}^{-1} \text{ sec}^{-1}$  and the resulting value of  $N$  for a thickness of  $0.15 \mu\text{m}$  is 0.006. This tends to support the original assumption of Newtonian cooling, although it should be borne in mind that the value of  $h$  from which it is derived assumes in the first place that Newtonian cooling applies.

The cooling rate in the regions which solidified into a non-crystalline structure must be significantly in excess of that for these lamellar crystalline areas. Such a cooling rate would be broadly consistent with estimates made by other workers for this technique. Ramachandrarao *et al* [10] obtained rates of the order of  $10^9 \text{ K sec}^{-1}$  from dendrite-arm spacing (DAS) measurements on a number of Al-Ge alloys but the cooling rate was not, apparently, sufficiently high to produce a non-crystalline phase. On the other hand, Ramachandrarao *et al* [2] reported a non-crystalline phase in eutectic Al-Ge alloy quenched on to a diamond substrate at 77 K, although a non-crystalline phase was not observed in eutectic Al-Cu alloy quenched under the same conditions and, presumably, subject to a com-

parable cooling rate. This implies that the cooling rate in the present Al-Cu non-crystalline phase must be greater than  $10^9 \text{ K sec}^{-1}$ , which supports the value calculated above.

### 3.3. Discussion of process mechanism of the technique

The fact that the present calculated value is higher than previous estimates suggests that careful attention to minimizing oxidation of the atomized liquid is an important factor. This may be effective in at least two ways; firstly, a reduction in oxidation on the particle surfaces would improve spreading on impingement with the substrate and, secondly, it would lead to more extensive wetting and improved thermal contact with the substrate. These effects were qualitatively confirmed by quenching experiments in argon atmospheres containing higher proportions of residual oxygen, i.e. with a higher residual air pressure in the vacuum chamber prior to filling with argon. The proportion of non-crystalline areas in a foil decreased as the nominal residual oxygen content of the atmosphere increased and, in the case of foils quenched in air, no evidence of a non-crystalline phase could be found. Moreover, in the latter case, fewer electron-transparent areas were present which could be interpreted on the basis of less efficient spreading of the liquid. Reduction in oxidation and water-vapour contamination of the surface of the copper substrate as a result of the sealed inert atmosphere may also be a factor in promoting efficient spreading of the liquid.

On first consideration and contrary to observation, one would expect that the ultimate controlling factor with regard to oxygen content of the splatting atmosphere would be the oxygen impurity content of the high and low pressure supplies from the cylinders, since for a purity of 99.999% there would be little point in evacuating the vessel below about  $10^{-2}$  Torr. However, continued evacuation below this pressure may be important in removing adsorbed oxygen and moisture from the inner walls of the vessel which, were evacuation to be terminated once the pressure reached  $10^{-2}$  Torr, might then desorb appreciably even after the vessel was charged with argon at 1 atm. Jansen [3] notes that the heated graphite crucible effects a considerable reduction in the partial pressure of oxygen in the vicinity of the sample and substrate.

In the samples quenched in the low-oxygen

environments, some structureless areas giving the non-crystalline diffraction pattern were also observed in chemically-thinned sections taken from thick sections at the centres of the foils. This suggests that the thinnest sections, at least, of some individual particles cool to below the glass-transition temperature for the alloy before succeeding particles arrive to be quenched on top of them. Calculations [11], assuming an average particle diameter of  $3 \mu\text{m}$  (which was observed experimentally for aluminium by Predecki *et al* [12]) and an even distribution of the particles, show that a cooling rate of greater than  $10^{10} \text{ K sec}^{-1}$  would be required in order that this could occur; this value is of the same order as that estimated above from the observed interlamellar spacing. The fact that the non-crystalline phase is formed at even higher rates of cooling in the thin sections at the edges then supports the possibility that it may also be present within the thicker sections of the splat. This has important implications with regard to the process mechanism of this technique since it follows that, if for some particles, at least, conditions of spreading and thermal contact are sufficiently favourable to give a cooling rate of  $10^{10} \text{ K sec}^{-1}$ , the effective thickness for the purposes of heat-transfer calculations should be that of individual spread-particles and not that of the final coalesced foil [9]. This situation differs from and is more complex than that, for instance, in the piston and anvil technique, where heat transfer is from a single droplet with a final thickness of some 30 to 50  $\mu\text{m}$ .

Calculations indicate that for an original individual particle diameter of  $3 \mu\text{m}$ , the final thickness should ideally, in the absence of oxide, be of the order of  $0.25 \mu\text{m}$  [11]. The individual spread particles at the edges of the splats shown in Fig. 4, are estimated to have had diameters of between  $0.25$  and  $0.3 \mu\text{m}$  before spreading and presumably these represent the extreme lower end of the particle size distribution. (Particles smaller than  $1 \mu\text{m}$  diameter, were not counted by Predecki *et al* [12].) These should, ideally, have spread to a thickness of about  $40 \text{ nm}$  [11]. Their thickness is estimated, however, to be somewhat greater than this, at between  $0.1$  and  $0.15 \mu\text{m}$ , which may be the result of the inhibiting effect of oxide. It is interesting to add that Ruhl [9] calculated that, for *ideal* cooling of a  $0.1 \mu\text{m}$  thick Fe splat on a Cu substrate at  $30^\circ\text{C}$ , the average cooling rate to half temperature would be  $8 \times 10^{11} \text{ K sec}^{-1}$ .

Another factor that may have an influence on the process is the time required for spreading in relation to the time required for cooling. At very high  $r$  and for the type of alloy where relatively little undercooling is possible, solidification could occur before spreading is complete. It is estimated [11] that for a cooling rate of  $10^{10}$  K sec<sup>-1</sup>, 3  $\mu$ m diameter particles would cool about 400 K during spreading (assuming spreading could be completed before solidification occurred) and 0.3  $\mu$ m diameter particles about 40 K (assuming, in both cases, the absence of surface oxide). The higher the rate of cooling the greater the amount of cooling during spreading, but on the other hand the more likely that the melt will undercool sufficiently to prevent freezing before spreading is complete. The structure or structures that will be obtained for a particular alloy will depend on the relative importance of many factors in addition to the purity of the inert environment and thermal and physical contact with the substrate – these include the average and minimum particle diameters, the amount of undercooling and the physical properties of the liquid alloy such as viscosity, surface tension and heat capacity per unit volume.

It is appropriate to comment on the microstructural methods for estimating the cooling rate. The fact that non-crystalline phases form at the very high cooling rates in both Al-Cu and Al-Ge alloys emphasizes the limitations of both the interlamellar spacing (ILS) and the dendrite-arm spacing (DAS) methods. The ILS method is probably subject eventually to greater restrictions than the DAS method since a normally two-phase eutectic alloy has a high probability of solidifying as one crystalline phase at very high cooling rates, though still below that required to form a non-crystalline phase, e.g. the Al-Cu system, where a single crystalline phase is formed at the intermediate cooling rates between lamellar and non-crystalline phase formation. Ideally, the type of alloy which would probably be applicable over the widest range of cooling rates using the DAS method would be a single-phase alloy having a fcc crystal structure, fcc components, a relatively low melting temperature and low activation energy for self-diffusion and viscous flow (see Section 3.5) for which the probabilities of forming a metastable, crystalline phase or a glassy phase were relatively low.

### 3.4. Non-crystalline phases in pure germanium and tellurium

By splat-quenching in argon on to the abraded copper substrate maintained at the temperature of boiling nitrogen and under carefully controlled conditions of substrate angle and liquid superheat, non-crystalline phases were produced in 99.999% pure germanium [13] and 99.999% pure tellurium [14]. The non-crystalline phases were present only in the thinnest sections of foils – generally the regions transparent to 100 kV electrons – although in some foils of Ge, the glassy phase was formed in sections which were just transparent to 1 MV electrons. As far as the present authors are aware the only previous case where a pure element has been produced in non-crystalline form by splat-quenching is boron [15]. For Ge, quenching on to a water-cooled substrate produced only the stable crystalline phase and only in about three-fifths of the quenches was the glassy phase produced, which suggested that the cooling rates attained in the present experiments were close to the critical value required for the solidification of Ge in glassy form. It was somewhat surprising that cooling the substrate to 77 K was necessary to produce this glassy phase since Ruhl [9] calculated that differences in substrate temperature in the range 300 to 77 K should have little effect on average cooling rate until the splat temperature had dropped below about 200°C. Preliminary heating experiments in the electron microscope indicate that the crystallization temperature for the glassy Ge phase is in the region 450 to 500°C and it would, therefore, be expected that its glass-transition temperature would be above 200°C and, hence, in the range where substrate temperature should ideally have little effect on cooling rate. Owing to the close proximity of the graphite crucible to the substrate, however, significant radiative heating of the substrate surface may be occurring when only water-cooling is employed, with a consequent decrease in cooling rate, in the temperature range of importance to glass formation, and liquid nitrogen cooling is possibly effective in reducing this heating.

In both cases, care was taken to quench from a temperature well below the melting point of the respective oxide – 1060°C for Ge compared with the melting point of GeO<sub>2</sub> (1116°C) and 560°C for Te compared with the melting point of TeO<sub>2</sub> (725°C) – since GeO<sub>2</sub>, at least, would inevitably solidify as a glass on quenching (a glassy phase

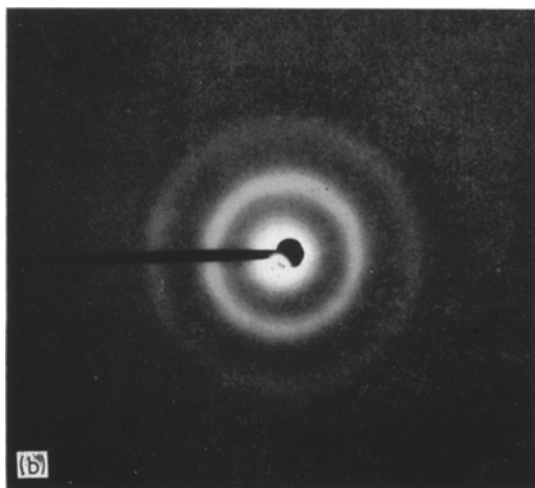
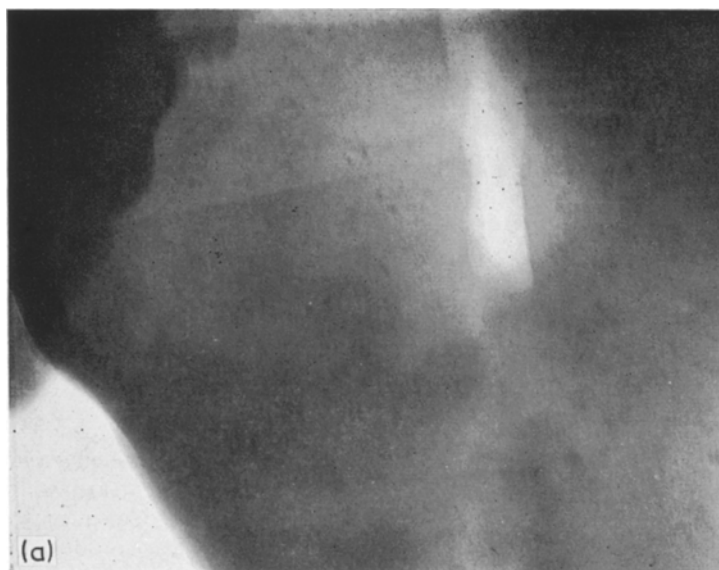


Figure 5 (a) Electron micrograph of non-crystalline phase in splat-quenched germanium ( $\times 60000$ ). (b) Electron diffraction pattern of the same area.

has also been reported in splat-quenched  $\text{TeO}_2$  [16]). The presence of only a minute quantity of glassy oxide could raise the possibility of confusion with the corresponding glassy pure elements.

The structures of the two non-crystalline phases were investigated by electron diffraction using 100 kV and 1 MV instruments. The peak positions of the diffraction pattern of the Ge phase (Fig. 5) were determined from microdensitometer traces and compared with those of

non-crystalline Ge, prepared by vapour deposition or sputtering, and those of liquid Ge [13]. Although there were variations from one sample to another of between  $\pm 3.5$  and  $\pm 5\%$  in the measured peak positions for the splat-quenched phase, the mean values for the 1st and 3rd peaks were in close agreement with those for vapour-quenched Ge (although agreement for the 2nd peaks was not so good); they differ substantially, however, from those for the liquid phase and, indeed, from those for glassy  $\text{GeO}_2$  (see Table I). There is experimental evidence to suggest that vapour-deposited, non-crystalline Ge has a short range, tetrahedral structure similar to that of crystalline Ge [17, 18]. In view of the similarity of their diffraction peak positions, it is probable that the splat-quenched and vapour-quenched phases have broadly similar structures, with perhaps detailed differences between them; it would follow, therefore, that the structure was not that of the "supercooled" liquid and that some short range structural rearrangement had taken place during cooling. The variations in peak positions from one sample to another were greater than would be expected from estimated errors in the measurements which suggests differences in the detailed structure of the phase, possibly as a result of variations in cooling rate.

The peak positions for the three visible electron diffraction rings of the splat-quenched glassy Te phase are given in Table II together with those for liquid Te, obtained by X-ray [19]



TABLE I Diffraction peak positions for non-crystalline splat-quenched and vapour-deposited Ge and for liquid Ge.  $K = 4\pi \sin \theta/\lambda$  ( $\text{\AA}^{-1}$ ).

Phase	1st peak	2nd peak	3rd peak
Splat-quenched Ge (e.d.)	1.89	3.05	5.34
Vapour-deposited Ge (e.d.)	1.89	3.32	5.23
Liquid Ge [30] (x-r.d.)	2.50	4.88	

Notes: e.d. – electron diffraction; x-r.d. – X-ray diffraction.

TABLE II Diffraction peak positions for non-crystalline splat-quenched Te, liquid Te and for splat-quenched Te-10% Ge alloy.  $K = 4\pi \sin \theta/\lambda$  ( $\text{\AA}^{-1}$ ).

Phase	1st peak	2nd peak	3rd peak
Splat-quenched Te (e.d.)	1.90	3.02	5.41
Liquid Te at 465°C (x-r.d.) [19]	2.06	3.16	4.40
Liquid Te at 575°C (n.d.) [20]	2.08	3.04	4.46
Splat-quenched Te-10% Ge (x-r.d.) [29]	1.97	3.30	5.26

Notes: e.d. – electron diffraction; x-r.d. – x-ray diffraction; n.d. – neutron diffraction.

and neutron-diffraction [20] and a splat-quenched amorphous Te-10% Ge alloy (X-ray diffraction) [29]. (Although a non-crystalline Te phase has also been produced by vapour-deposition at liquid nitrogen temperature, this was reported to be unstable at ambient temperature [21] and no report of an investigation of its structure could be found in the literature.) The first peak for the splat-quenched Te, which often crystallized readily in the electron beam and rendered observations difficult, lies at a somewhat smaller angle than that for the liquid phase which implies a longer nearest neighbour distance in the former. The second peak position is in close agreement with that for the liquid phase but the third peak occurs at a substantially higher angle than that for the liquid though it is similar to the third peak position for the Te-10% Ge alloy. It appears, therefore, that the splat-quenching process caused some short-range rearrangement in the mean atomic positions from those that prevail in the liquid state though probably not as much as in the case of the non-crystalline splat-quenched germanium. It is perhaps not surprising that there should be less structural change during quenching for Te than for Ge since liquid Te has, even up to 100°C above its freezing point, a very open structure with a co-ordination number of 2, as is found in crystalline Te [19], whereas liquid Ge has a more close-packed metallic structure, with a co-ordination number in the range 6 to 8.

With the semi-quantitative photographic plate and microdensitometer techniques employed

here, it is only possible to speculate on the detailed structure of the splat-quenched Ge and Te phases and a device to filter out inelastically scattered electrons would be required to permit a radial distribution analysis by Fourier transformation before firm conclusions could be drawn.

### 3.5. Metallic glass formation

The conditions for metallic glass formation are not clearly established but the temperature dependence of viscosity of the liquid phase, and hence the activation energy for diffusion, at high degrees of undercooling plays an important part [22]. One can only speculate on the relative behaviour of this property for pure elements and alloys at high degrees of undercooling by considering the relative behaviour in their stable liquid ranges. Many of the alloys which have been splat-quenched into an amorphous or microcrystalline form are based on metals which have relatively high activation energies for viscous flow,  $E$ , [23], such as noble and transition metals – in particular Fe and Ni (this has been noted previously by Cahn [24]). Although viscosity data are not available for liquid Pd and Pt, many alloys of which also readily solidify into a non-crystalline form, we may suppose that, as transition metals, they also have high values of  $E$ . Pure aluminium, although it is a low melting point metal, also has a fairly high value of  $E$  ( $\sim 16.7 \text{ kJ mol}^{-1}$ ), of the same order as that of pure gold, which may partly explain why it has been possible to produce glassy phases in two

of its alloys. The values for liquid Ge [25] and Te [26] are 27.6 and 21.2 kJ mol<sup>-1</sup>, respectively (the former being derived from liquid self-diffusion data); these are again relatively high, which probably partly explain their behaviour on quenching, although their high entropies of fusion, and hence of transformation from glass to crystal, would also be expected to contribute to the high stability of the glassy phases.

It is also noteworthy that of the several metals [27, 28] that have been vapour-quenched into a non-crystalline form, nickel is one of the few having a close packed crystal structure which appears to be stable at room temperature. Moreover, of all the metals whose viscosities have been investigated experimentally, nickel has the highest value of  $E$  and it is interesting to speculate that glassy Ni could eventually be produced by this splat-quenching technique.\*

#### 4. Summary

An apparatus for splat quenching by the gun technique has been constructed whereby quenching can be performed in a sealed atmosphere of inert gas. The reduced oxidation of the atomized liquid droplets during quenching leads to more efficient spreading of the droplets on impact with the substrate and to improved thermal contact. An estimate of the cooling rate of individual droplets, in a quenched Al-17.3 at. % Cu eutectic alloy having original diameters of the order of 0.25  $\mu\text{m}$ , was made from the spacing of the lamellae in the spread and frozen droplets; this gave a value of  $\sim 10^{10}$  K sec<sup>-1</sup> which is higher than previous estimates for splat-quenching techniques.

New non-crystalline phases were produced in the thinnest regions of quenched foils of the Al-17.3 at. % Cu alloy, pure Ge and pure Te. The selected-area electron diffraction patterns from these areas were compared, where possible, with diffraction peak positions from corresponding liquid- and vapour-deposited phases. The position of the first broad maximum for the Al-Cu phase corresponds roughly with the (111) peak for the single phase crystalline alloy.

Lattice image studies suggest that the glassy Al-Cu phase has an amorphous rather than microcrystalline structure. The mean peak positions for the splat-quenched Ge phase are broadly in agreement with those for vapour-deposited Ge and are substantially different from

those for liquid Ge. This suggests that considerable atomic rearrangement took place during cooling and freezing of the Ge and that the splat-quenched glassy phase may have a paracrystalline, tetrahedral short-range structure. Not surprisingly, the peak positions for glassy splat-quenched Te bear a much closer resemblance to those of the liquid phase than is the case for Ge, suggesting that the low co-ordination, paracrystalline structure of liquid Te is largely preserved on splat-quenching. However, no definite conclusions can be drawn regarding the detailed structures from these semiquantitative comparisons of peak positions.

The occurrence of the glassy Al-Cu phase within thick sections of quenched foils and the observations of individual spread particles only 0.3  $\mu\text{m}$  in diameter at least partly invalidate assumptions that have previously been made about the particle size distribution and effective thickness for heat-transfer calculations.

#### Acknowledgements

The authors are grateful to Professor G. W. Greenwood for providing laboratory facilities, Messrs M. Parry and H. Turner for valuable technical assistance, Dr L. Gillott of the Physics Department, Sheffield University for preparing vapour-deposited and sputtered films of Ge, Dr G. Tourand, Saclay for providing neutron diffraction data for liquid Te and Mr F. Sheldon of the Applications Laboratory, Pye-Unicam Ltd, for providing facilities for and helpful assistance with high-resolution electron microscopy. They also wish to acknowledge the financial support of the Science Research Council and the use of the SRC/BSC 1 MV electron microscope facility at Swinden Laboratories, Rotherham.

#### References

1. P. DUWEZ and R. H. WILLENS, *Trans. Met. Soc. AIME* **227** (1963) 362.
2. P. RAMACHANDRARAO, M. LARIDJANI and R. W. CAHN, *Z. Metallk.* **63** (1972) 43.
3. C. H. JANSEN, Ph.D. Thesis, MIT (1971); J. VITEK and N. J. GRANT, *J. Mater. Sci.* **7** (1972) 1343.
4. T. TAKAMORI and R. ROY, *ibid* **8** (1973) 415.
5. M. H. BURDEN and H. JONES, *J. Inst. Metals* **98** (1970) 249.
6. H. A. DAVIES and J. B. HULL, *Scripta Met.* **6** (1972) 241.

\*We have now succeeded in splat-quenching pure nickel into a non-crystalline form. Details of this are given elsewhere [31].

7. A. REVCOLEVSCHI and N. J. GRANT, *Met. Trans.* **3** (1972) 1545.
8. A. HOWIE, O. KRIVANEK and M. L. RUDEE, Proc. 5th Eur. Cong. Electron Microscopy (Institute of Physics, London, 1972) p. 450.
9. R. C. RUHL, *Mat. Sci. Eng.* **1** (1967) 313.
10. P. RAMACHANDRARAO, M. G. SCOTT and G. A. CHADWICK, *Phil. Mag.* **25** (1972) 961.
11. H. A. DAVIES, to be published.
12. P. PREDECKI, A. W. MULLENDORE and N. J. GRANT, *Trans. Met. Soc. AIME* **233** (1965) 1581.
13. H. A. DAVIES and J. B. HULL, *Scripta Met.* **7** (1973) 637.
14. J. B. HULL and H. A. DAVIES, to be published.
15. F. GALASSO, R. VASLET and J. PINTO, *Appl. Phys. Letters* **8** (1966) 331.
16. P. T. SARJEANT and R. ROY, *J. Amer. Ceram. Soc.* **50** (1967) 500.
17. H. RICHTER and O. FÜRST, *Z. Naturforsch.* **6a** (1951) 38.
18. T. B. LIGHT, *Phys. Rev. Letters* **22** (1969) 999.
19. R. C. BUSCHERT, Ph.D. Thesis, Purdue University (1957).
20. G. TOURAND, private communication.
21. Y. SHI-TUAN and A. R. REGEL, *Sov. Phys. Solid State* **3** (1962) 2627.
22. D. R. UHLMANN, *J. Non-Cryst. Solids* **7** (1972) 337.
23. R. T. BEYER and E. M. RING, "Liquid Metals", edited by Z. Beer (Dekker, New York, 1972) p. 431.
24. R. W. CAHN, *Fizika* **2**, Suppl. 2 (1970) 25.1.
25. P. V. PAVLOV and E. V. DOBROKLOMOV, *Fiz. Tverd. Tela* **12** (1970) 281.
26. Y. NAKAMURA and M. SHIMOJI, Trans. 2nd Int. Conf. Props. Liq. Metals. Tokyo, (Taylor and Francis, London, 1973) p. 567.
27. S. FUJIME, *Jap. J. Appl. Phys.* **5** (1966) 764, 778, 1029; **6** (1967) 305.
28. J. R. BOSNELL, *Thin Solid Films* **3** (1969) 233.
29. H. L. LUO and P. DUWEZ, *Appl. Phys. Letters* **2** (1963) 21.
30. H. HENDUS, *Z. Naturforsch.* **2a** (1947) 505.
31. H. A. DAVIES, J. AUCOTE and J. B. HULL, *Nature, Physical Science*, **246** (1973) 13.

Received 21 August and accepted 26 September 1973.